

ECE 445
SENIOR DESIGN LABORATORY
FINAL REPORT

Automatic Page-Turning Photocopier

Team #4

YINGYING GAO
(yg24@illinois.edu)
YIYING LYU
(yiyingl3@illinois.edu)
XUAN ZHU
(xuanzhu5@illinois.edu)
SHUCHANG DONG
(sdong19@illinois.edu)

TA: Yun Long

May 16, 2025

Abstract

This report introduces a photocopier system which can turn pages automatically. The system features a mechanical structure for precise page handling paired with a camera adaptive LED lighting to capture clear images and a user interface for real-time operation monitoring. It integrates subsystems including a page-turning mechanism ensuring single-page flipping within sixteen seconds, a photocopying unit optimized for varied paper textures through a control panel enabling preset commands and progress tracking. Success metrics focus on flawless single-page accuracy consistent cycle times and automatic shutdown post-task completion. Testing demonstrates the system efficiently processes bound and stapled materials while maintaining scan clarity and operational speed. This innovation cuts manual intervention with a success rate higher than 75 % and improves consistency in archival or bulk scanning tasks. Future enhancements will target scalability for materials in greater size and energy efficiency improvements.

Contents

| | | |
|----------|--|-----------|
| 1 | Introduction | 1 |
| 1.1 | Background and Objective | 1 |
| 1.2 | Block Description | 1 |
| 1.3 | High-Level Requirements List | 2 |
| 2 | Design | 3 |
| 2.1 | Design Procedure | 3 |
| 2.1.1 | Page-Turning Module | 3 |
| 2.1.2 | Image Processing Module | 3 |
| 2.1.3 | Control Module | 3 |
| 2.2 | Design Details | 4 |
| 2.2.1 | Page-Turning Module | 4 |
| 2.2.2 | Image Processing Module | 7 |
| 2.2.3 | Control Module | 8 |
| 2.2.4 | Power Supply Module | 10 |
| 3 | Design Verification | 11 |
| 3.1 | Page-Turning Module | 11 |
| 3.1.1 | Mechanism | 11 |
| 3.1.2 | Base Frame | 12 |
| 3.2 | Image Processing Module | 13 |
| 3.2.1 | User Interface | 13 |
| 3.2.2 | Image Processor | 14 |
| 3.2.3 | Camera | 14 |
| 3.3 | Control Module | 14 |
| 3.3.1 | Motor Driver | 14 |
| 3.3.2 | UART Transmission | 15 |
| 3.3.3 | Photoelectric Sensor | 16 |
| 3.3.4 | Emergency Stop | 17 |
| 4 | Costs | 18 |
| 5 | Schedule | 19 |
| 6 | Conclusion | 20 |
| 6.1 | Accomplishments | 20 |
| 6.2 | Uncertainties | 20 |
| 6.3 | Ethical considerations | 20 |
| 6.4 | Future Work | 20 |
| | References | 21 |

1 Introduction

1.1 Background and Objective

Photocopiers are the most useful tool in our life, particularly in school, bookstore, library, etc. However, traditional photocopiers designed for bound materials, such as books or manuals, often require manual page turning, leading to inefficiency and user fatigue. Repetitive handling can also result in human error and potential damage to delicate materials, such as antique books or blueprints. To address these challenges, an automated solution is needed to streamline the scanning process while ensuring precision and care for various types of documents.

This project aims to revolutionize document scanning by addressing the inefficiencies of traditional photocopiers when handling bound materials, which typically require manual page-turning, leading to slower processing times, increased labor costs, and human error due to fatigue. By developing an automatic page-turning photocopier, we seek to eliminate manual intervention, enhance accuracy, and preserve delicate materials, such as antique books and blueprints, through gentle robotic handling. Additionally, our compact and cost-effective solution improves accessibility while enabling seamless digitization by capturing high-quality images and converting text into editable digital formats. Ultimately, this innovation will save time, reduce manual effort, and minimize wear and tear, benefiting industries ranging from libraries and archives to engineering firms and offices.

1.2 Block Description

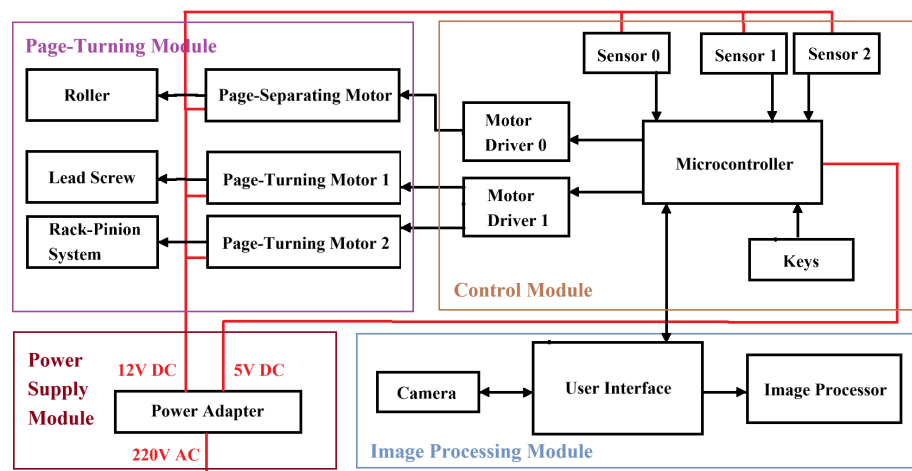


Figure 1: Block Diagram

To achieve the function, four subsystems are required in the whole design as illustrated in Figure 1.

- **Power Supply Module:** The power supply module connects the other three modules and provides power with proper voltage. The control section is powered via a 5 V supply from the host PC. The motors and optical sensors are powered by a dedicated 12 V DC power source, which is derived from a step-down transformer connected to a 220 V AC power source.
- **Page-turning Module:** The page-turning module has two mechanisms: page separation and page moving mechanism. A motorized roller system employs a chain transmission to rotate a cylindrical drum to curl and separate the pages. The lead screw would make linear movement and a rack-and-pinion system is responsible for the page-turning motion.
- **Image processing Module:** The image processing module consists of a camera, user interface, and image processor. It is responsible for accurately reproducing the content of pages by capturing high-resolution images, processing them for clarity, and sending the final output.
- **Control Module:** The control module uses STM32F407 microcontroller to receive and send signals to connect the page-turning module and image processing module.

1.3 High-Level Requirements List

- The system must complete a single page-turning cycle within 16 seconds. This is measured from the moment a page is detected to the successful completion of the page flip. The efficiency of the automatic page-turning photocopier will be evaluated by averaging the time taken over 10 consecutive operations.
- This photocopier is required to produce scanned images with no significant shadows or reflections. This will be assessed by evaluating the page area affected by such artifacts under standard testing conditions.
- The mechanism must be capable of handling documents with varying binding types and thicknesses. Its performance will be validated by ensuring successful handling of $\geq 90\%$ of bound materials without causing tearing or misalignment during operation.

2 Design

2.1 Design Procedure

2.1.1 Page-Turning Module

We choose to use a purely mechanical structure instead of controlling the robotic arm to reduce the volume and mass of the page-turning device and achieve the design advantages of a small footprint and portability. The joint motion of the mechanical structure controlled by three motors can be simulated and visualized in SolidWorks, shown in the right part of Figure 2. The reason for using gear and chain to control the rotation of the roller is that it is convenient for fine-tuning the relative position of the roller and the motor. Using a lead screw to control the advancement of the insert is because it can more precisely control the relative position to the paper surface. The reason for using gear and rack to control the left and right page-turning of the insert is that it is faster.

2.1.2 Image Processing Module

For the user interface, we chose to implement a software-based UI using Qt. Alternative approaches we considered included using a physically embedded touchscreen or implementing a web-based interface accessible via a browser. While an embedded screen could provide a compact, all-in-one solution, it would significantly increase hardware complexity and cost. A web-based interface would introduce additional networking and browser compatibility concerns. Qt offers a flexible and visually rich framework for desktop applications, supports cross-platform development, and allows for rapid prototyping and customization. This made it an ideal choice for our project, as it enabled us to build an intuitive and responsive interface without the overhead of additional hardware or complex deployment setups.

2.1.3 Control Module

We select STM32F407 [5] as the microcontroller due to its high-performance Cortex-M4 core, rich peripheral set, and excellent real-time control capabilities. It offers multiple timers for precise PWM generation, provides sufficient GPIO and interrupt channels for responsive sensor integration, and supports advanced interfaces for future usage. Its balance of computational power, flexibility, and community support makes it well-suited for managing the coordination required in an automatic page-turning and scanning system.

As for motor drivers, we initially chose CCM2 speed regulators for motors. However, the direction output of this motor driver cannot be controlled by the microcontroller. Thus, we eventually employ an L298N dual H-bridge driver for motor control.

Rather than designing constant-time movements for motors, we employ photoelectric sensors to ensure precise and reliable control over the motors during operation.

2.2 Design Details

Based on the design procedure, we can then describe every part in detail and the specific requirements are listed in Table 8, Table 9 and Table 10.

2.2.1 Page-Turning Module

This module has two mechanisms: page separation and page moving mechanism. For the page separation system, a motor-driven roller system employs a chain transmission to rotate a cylindrical drum. The rotation creates friction between the drum surface and the target page, enabling controlled curling and separation from adjacent pages through this frictional engagement. The page moving mechanism is a 2 DOF structure. A lead screw drives the page-turning strip move forward to insert its tip into the created inter-page gap. Moreover, via a rack-and-pinion system, the mechanism enables lateral movement across the book plane, completing the page-flipping motion by carrying the separated page to the opposite side. The cooperation between these two mechanisms enables page-turning automation through sequential page separation and guided translocation. Three photoelectric sensors are used to detect the status of the operation progress of each part of the system. When the page is rolled up by the roller, the photoelectric signal of the sensor will be blocked by the bent page. At this time, the control module will stop the motor that controls the roller from rotating and trigger the motor to turn the lead screw to make the strip move forward and insert into the gap between the pages. After it is fully inserted, the motor will drive the gear-rack transmission to control the strip to turn the page. When the page-turning action is completed, the rack reaches the specified position and is recognized by the sensor. Then the control module will trigger the motor to move in the reverse direction so that all components return to their original positions.

Figure 2 shows the whole page-turning mechanism and the camera. The area of the page-turning part is 40 cm, and the maximum height is about 60 cm which is the height of the camera. For most of the parts, we use standard components. The aluminum profile is used to build the base which connects all assembly parts.

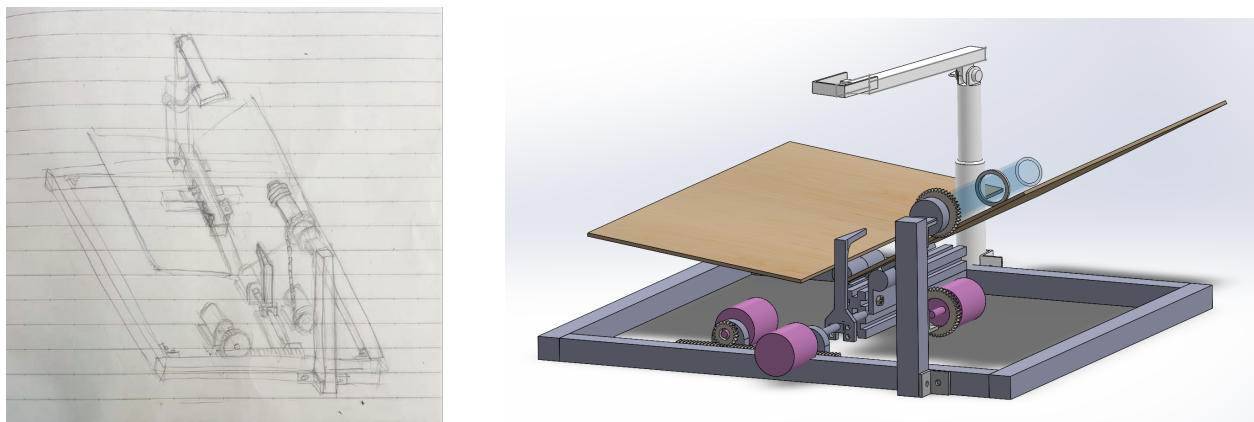


Figure 2: Mechanism Sketch

The number of motor revolutions required to move the lead screw by a certain distance is calculated as:

$$N = \frac{d}{L} = \frac{30mm}{1.2mm} = 25 \quad (1)$$

where d is the linear displacement of the lead screw, L is the lead of the screw (i.e., the distance the nut moves per revolution), and N is the number of motor revolutions.

The relationship between the linear displacement of the rack and the number of motor rotations is given by:

$$N = \frac{d}{2\pi r} = \frac{64.6mm}{2\pi * 15mm} = 0.685 \quad (2)$$

where d denotes the displacement of the linear motion, r represents the radius of the gear, and N indicates the number of rotations (cycles) driven by the motor.

The overall physical diagram of the page-turning part is shown in Figure 3. It can be seen that the book placed on the base frame is very compatible with other mechanical structures.

The base Frame is constructed with aluminum profiles to form a rectangular foundation frame, providing rigidity and lightweight support. The book platform consists of two large acrylic sheets (\geq A3 size) connected via hinges, enabling angular adjustment which is designed to prevent text distortion through optimal plane alignment. The adaptive supporter for the camera is assembled on a rectangular foundation frame.

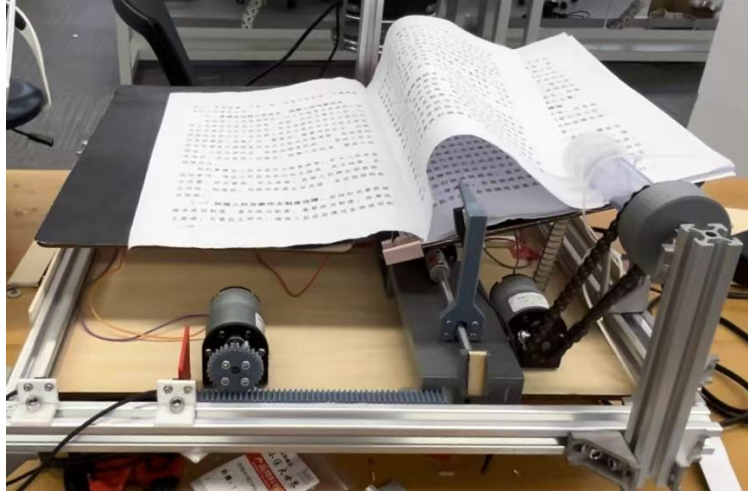


Figure 3: Physical diagram

One significant tolerance we need to consider is the page friction problem. Since our goal is that only one page can be turned at one time, we should make sure that the mechanism structure meets this requirement. Based on the free-body diagram, we can list the equations below:

$$N_1 = mg\cos(\theta) + F\cos(\theta) \quad (3)$$

$$f_r = \mu_r N_1 + F \cos \theta \quad (4)$$

$$N_2 = mg \cos(\theta) + N_1 \quad (5)$$

$$f_{p1} = \mu_p N_2 \quad (6)$$

$$N_3 = mg \cos(\theta) + N_2 \quad (7)$$

$$f_{p2} = \mu_p N_3 \quad (8)$$

Where:

θ is the angle between the book supporter and the ground;

μ_1 is the friction coefficient between a page and the silicone ring;

μ_2 is the friction coefficient between adjacent pages;

m is the mass of one page, $m = 3.52 \text{ g}$;

g is the gravitational acceleration, $g = 9.81 \text{ m/s}^2$;

λ is the proportion of the contact area between two adjacent sheets of paper;

F is the force applied by the silicone ring.

To make sure the first page can be motivated, we have this relationship:

$$f_r > f_{p1} - mg \cos(\theta) + F_p - F \sin(\theta) \quad (9)$$

Where F_p is the force required to bend the page, $F_p = 0.0205 \text{ N}$. And to make sure the other pages stay unmoved, we have this relationship:

$$f_{p1} > f_{p2} - mg \sin(\theta) + F_p \quad (10)$$

The range of F and frac can be obtained by varying the value of the other variables. Thus, the proportion of the contact area between two adjacent sheets of paper should be greater than 80%. For most common cases, we assume the average proportion value is 0.9. Then we can get the range of force that $0.0739 \text{ N} \leq F \leq 0.1 \text{ N}$. In this case, the force range is $0.09 \text{ N} \pm 0.01 \text{ N}$ ($\pm 11\%$). In conclusion, the tolerance for the force acting on a page is 11%.

Based on the information about the friction force on the paper surface and the pressure that the roller needs to provide, we can further simulate and analyze the stress and deformation of the roller. Since the roller is subjected to complex forces and plays an irreplaceable role in the page-turning process, it is very important to conduct a separate stress-strain analysis on it. From Figure 4 a), the main forces acting on the drum can be seen, including the support force and friction force from the outermost paper surface on the right side, the pulling force provided by the cable tie, the pulling force provided by the chain, and the balancing force provided by the fixed bearing. Figure 4 b) shows the stress distribution of the roller. It can be found that the stress is mainly concentrated at the bearing connection because the radius of the connection part is very small. The calculated maximum Von Mises Stress is $1e8 \text{ N/m}^2$, which is within the acceptable range. Figure 4 c) shows the overall deformation displacement of the roller. It can be observed that the outermost end of the roller will tilt downward, so as to press the pages tightly.

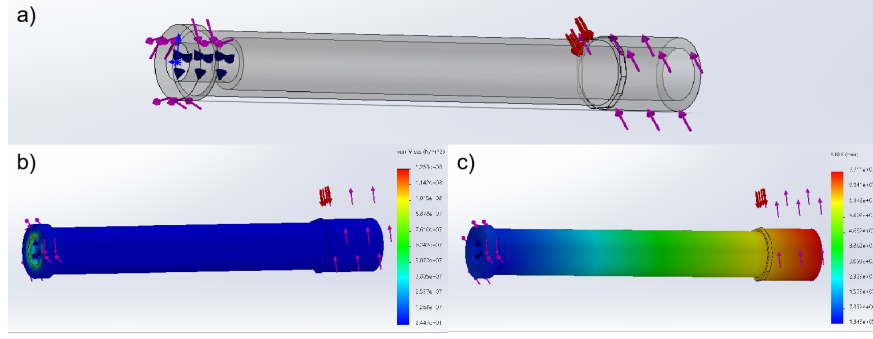


Figure 4: Simulation of Roller Drum

2.2.2 Image Processing Module

The image processing module is responsible for capturing images, processing them for clarity, and interacting with users. It consists of a camera, user interface, and image processor. Once the mechanical system turns the page, the camera captures a high-resolution image of the exposed page. The captured image is then transmitted to the image processor, which enhances the content and stores the results. Figure 5 shows an overview of this module.



Figure 5: Schematic Diagram

The Camera captures high-quality images of book pages during the scanning process. It features a resolution of 1920×1080 pixels, which is specifically chosen to allow simultaneous capture of two facing pages of an open book. This high-resolution capability ensures that the text on both pages is clearly identifiable and legible, preserving fine details such as small fonts, intricate diagrams, or faded print that may be present in antique or fragile documents.

The Image Processor is a Python program that refines the raw images captured by the camera. It begins by detecting the edges of the two facing pages in the image (received via USB from the Camera) and crops them into two separate page images. It then performs page dewarping to correct distortions caused by the curvature of bound books, producing flat, readable pages. The image processing techniques are based on an online article [4]. The page dewarping algorithm is based on a Python package [2][3]. The processed images are stored automatically and made accessible to users through the User Interface, enabling easy viewing and retrieval of high-quality scanned content. Figure 6 shows the original captured image, and Figure 7 shows the processed result.

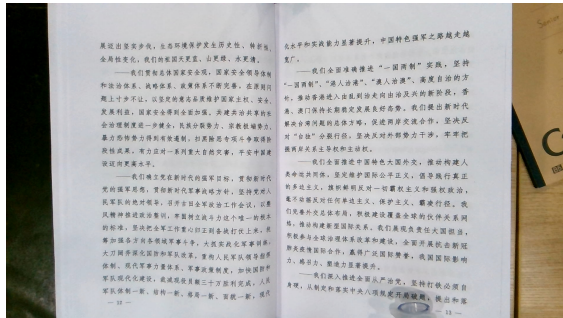


Figure 6: Original Captured Image

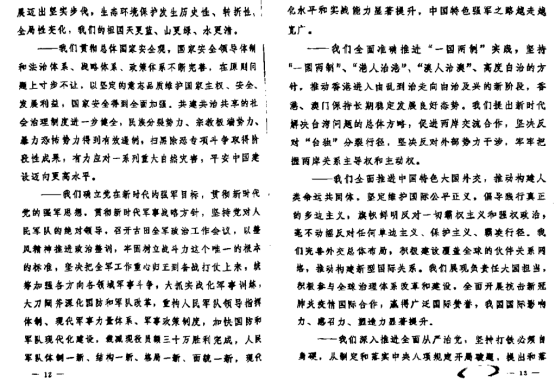


Figure 7: Processed Image

The User Interface (UI) serves as the central control panel for the automated book scanner, allowing users to easily operate the system and manage scanned content. It provides two scanning modes: Quick Start Mode for immediate scanning with a single click, and Range Mode, which lets users specify the number of page turns to automate scanning of multiple pages in sequence. Users can select the page size (e.g., B5), start or stop the system, and view both captured photos and processed images. The UI also allows users to run the Image Processor directly, ensuring a seamless transition from capture to processing. A status display keeps users informed of the system's current state, enhancing usability and operational feedback. Figure 8 demonstrates the User Interface layout.

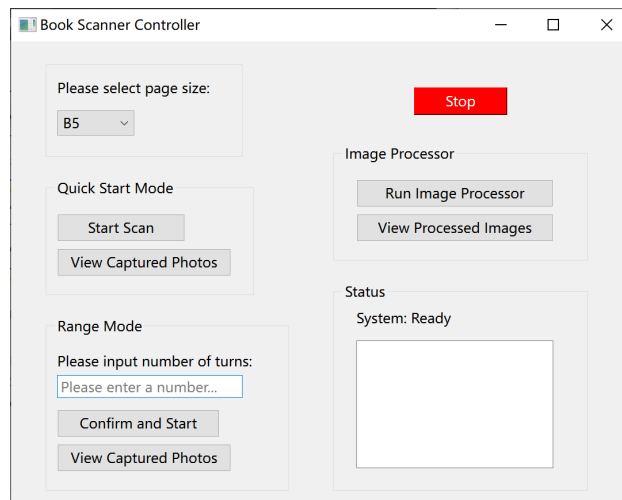


Figure 8: User Interface

2.2.3 Control Module

The control module serves as the central coordinator of the entire system. It builds around a microcontroller (STM32F407) and consists of two motor drivers, three photoelectric sensors, and four external keys. It is responsible for orchestrating motor control, sensor input

processing, user interaction, and communication with the image processing module. The microcontroller schematic is shown in Figure 14 and Figure 17.

As for controlling three motors, the microcontroller receives GPIO input signals from photoelectric sensors and generates PWM and GPIO output signals for motor drivers. The page-separating motor is driven through one channel of an L298N dual H-bridge driver, and the two page-turning motors are each driven through one channel of another L298N driver, as shown in Figure 15. The microcontroller receives feedback from three photoelectric sensors. An EX-13A photoelectric through-beam sensor is used to detect successful page separation. Two EX-14A photoelectric diffusion-reflective sensors are used to detect the position of the rack-pinion system during operation. The workflow is shown in Figure 9.

The microcontroller establishes UART-based serial communication with a host PC via the CH340 interface to interact with the user interface, as shown in Figure 16. It receives commands like START, as well as personalized presetting, including page size and number of page-turning cycles. The external interrupt command STOP sent by the host PC will invoke an interrupt service routine that immediately disables all motor PWM outputs and stops ongoing processes.

The microcontroller also receives GPIO input signals from four external keys to set the initial position of the lead screw and the rack-pinion system before operation.

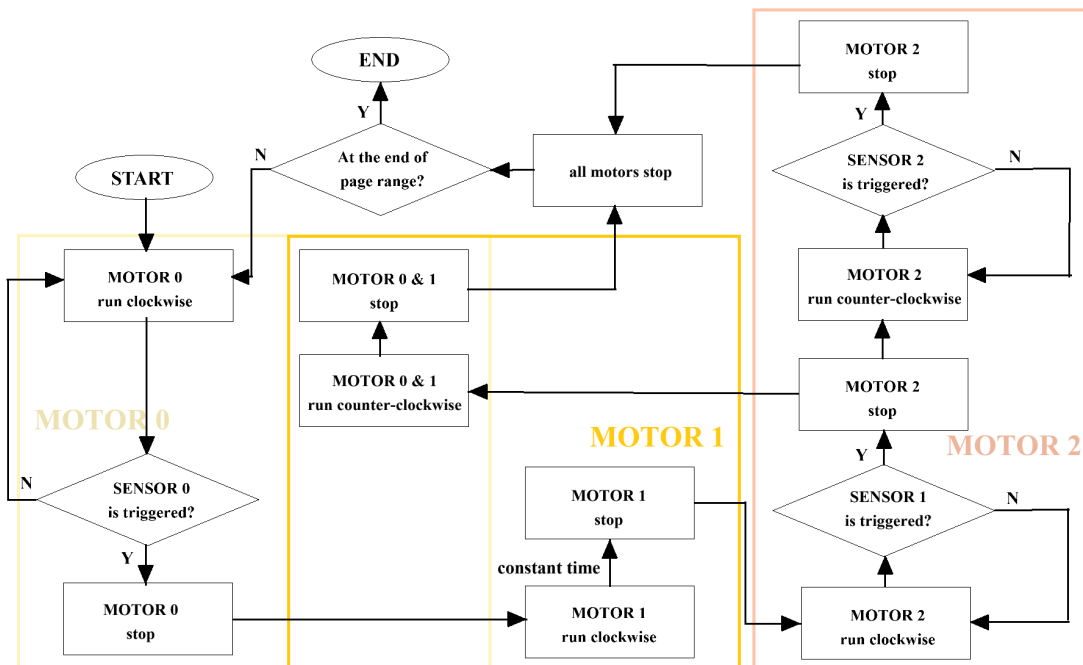


Figure 9: Workflow of Motor Controlling

2.2.4 Power Supply Module

The power supply module is divided into two coordinated sections: a low-voltage control circuit and a high-current actuator circuit. Both are provided by a power adapter connected to a 220 V AC power source.

The control section is powered via a 5 V DC source. This 5 V DC input is regulated on the PCB by an onboard low-dropout voltage regulator to provide a stable 3.3 V supply for the microcontroller and other low-power peripherals.

The motors and photoelectric sensors are powered by a 12 V DC power source.

Although the voltage domains are separated to ensure proper power distribution, both sections share a common ground to maintain signal integrity and ensure reliable logic-level interfacing between the microcontroller and external devices.

3 Design Verification

Detailed requirements and verification can be found in Table 8, Table 9 and Table 10.

3.1 Page-Turning Module

3.1.1 Mechanism

We used a camera to record multiple consecutive processes to verify the time required for each cycle of the page-flipping photocopying work. By reading the start and end times of each stage, we can obtain the average time required for one cycle. Based on the video screenshots and time shown in Figure 10, we have obtained that the average time required for one cycle of page-flipping photocopying is 14 seconds.

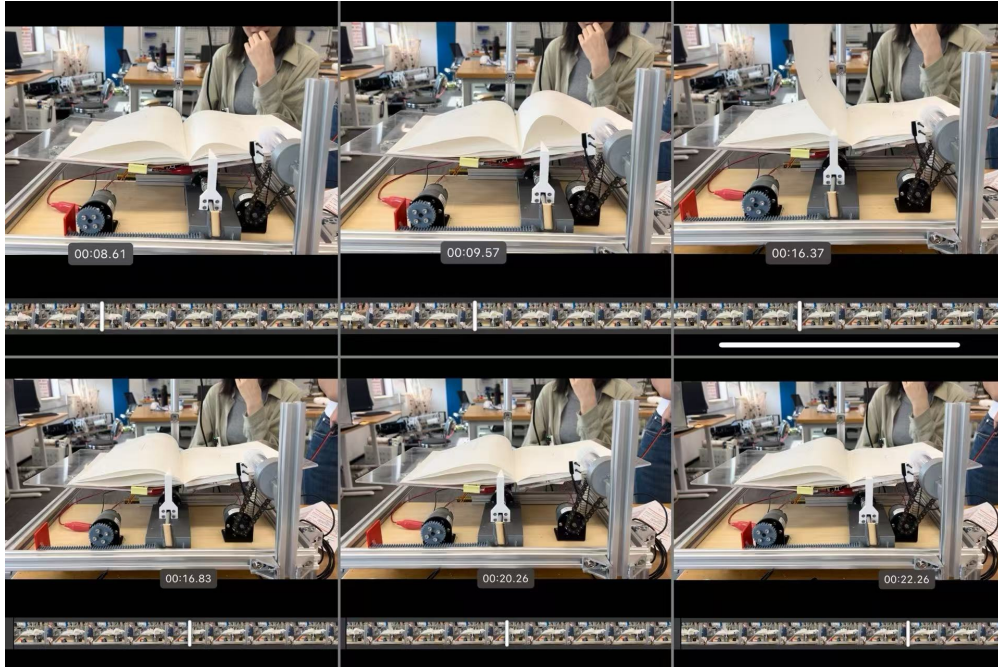


Figure 10: Whole Cycle with Time Label

We did experiments on the cycle time for the B5 size document. We did it 5 times in total and each time we turned 5 pages and recorded the videos. Then we read the cycle time from the videos and calculated the mean cycle time. The data is shown in Table 1.

For the B5-sized bound notebooks, we conducted a flipping test of four consecutive sets of five pages each, totaling 20 flips. Based on the average calculation, the ratio of the successfully flipped pages to the total number of flips is approximately 83%. To verify the success rate of the page-turning module, we did 10 times experiments. We turned 10 pages each time to calculate the success rate for each experiment and the mean success rate, which is shown in Table 2. The successful flipping rate of the thicker bound books is also basically similar. When the roller comes into contact with the pages of the book,

Table 1: Cycle Duration Test Result

| Group | Cycle 1 | Cycle 2 | Cycle 3 | Cycle 4 | Cycle 5 | Mean |
|-------|---------|---------|---------|---------|---------|--------|
| 1 | 14 s | 14 s | 15 s | 14 s | 14 s | 14.2 s |
| 2 | 14 s | 14 s | 14 s | 15 s | 15 s | 14.4 s |
| 3 | 14 s | 14 s | 14 s | 14 s | 14 s | 14 s |
| 4 | 14 s | 14 s | 14 s | 14 s | 14 s | 14 s |
| 5 | 14 s | 14 s | 14 s | 15 s | 16 s | 14.6 s |

the problem of multiple pages being turned only occurs when turning the first page. This is due to the excessive pressure exerted by the roller on the page. This problem does not occur in the process of turning the subsequent pages.

Table 2: Success Rate Test Result





| Experiment No. | 1 | 2 | 3 | 4 | 5 | 6 | 7 | 8 | 9 | 10 | Mean |
|------------------|----|----|-----|----|----|----|-----|----|----|----|------|
| Success Rate (%) | 80 | 60 | 100 | 60 | 90 | 80 | 100 | 80 | 90 | 90 | 83 |

For stapled A4 documents, the page-turning success rate is slightly lower than that of B5, with an approximate success rate of around 75%. This is because A4 printing paper is stiffer and more brittle, and random creases and wrinkles will appear on the paper surface due to uneven stress. During the process of the strip pushing the page, although the base of the page moves a certain distance, it cannot be turned over to the other side smoothly as a whole. Generally speaking, increasing the moving distance range of the strip can effectively solve this problem. Currently, the position of the motor in the aluminum profile frame limits the range of rack and pinion transmission. To increase the movement distance of the strip, the position of the motor in the frame needs to be adjusted. At present, the simplest solution is to place the motor under the horizontal template.

3.1.2 Base Frame

We selected four types of bound materials with varying sizes and weights for testing. All four materials were able to avoid page distortion and occlusion by adjusting the hinge angle. In addition, we measured the deformation of the planar support rod, as well as the change in the inclined surface angle under prolonged maximum load conditions (i.e., the gravitational force of each bound material). Table 3 reflects the degree error for four different types of materials.

Table 3: Material Test

| | | | | |
|--------------|---|---|--|---|
| Materials |  |  |  |  |
| Mass | 340.1 g | 228.1 g | 524.4 g | 181.5 g |
| Deformation | 0 mm | 0 mm | 0 mm | 0 mm |
| Degree error | 1° | 0° | 2° | 0° |

3.2 Image Processing Module

3.2.1 User Interface

The user interface was tested to ensure it meets key functional requirements, including real-time system status updates and responsive operations upon user input.

For the “Start Scan” and “Stop” buttons, ten test cycles were performed with randomized delays between button presses, and system timestamps were used to measure response intervals. All responses were within 1 s, with an average response time of 550 ms and a maximum observed delay of 720 ms.

The “Run Image Processor” button was verified by executing the processor with ten test cycles, each with 5 test images. The output was checked in the designated output directory. In all test cases, the system correctly generated processed images with no data corruption, validating that the user interface properly triggers the image processing workflow.

To ensure the system accurately turns the specified number of pages, tests were conducted with inputs of ten different page turns (1–10). The system achieved 100% accuracy in all the tests. This confirms that the user interface correctly relays user input to the page-turning mechanism without errors.

The ability of the user interface to display real-time status updates was verified by triggering three different system state changes for ten test cycles. While the requirement specifies a 500 ms maximum latency, precise instrumentation was unavailable for exact measurement since the latency is too small. However, in all test cases, updates appeared immediately to human perception, with no observable delay. Given this qualitative assessment, the system likely meets the timing requirement, though future validation with proper timing equipment is recommended for absolute confirmation. Figure 11 demonstrates the user interface of three system states—Ready, Scanning, and Running Python Script.

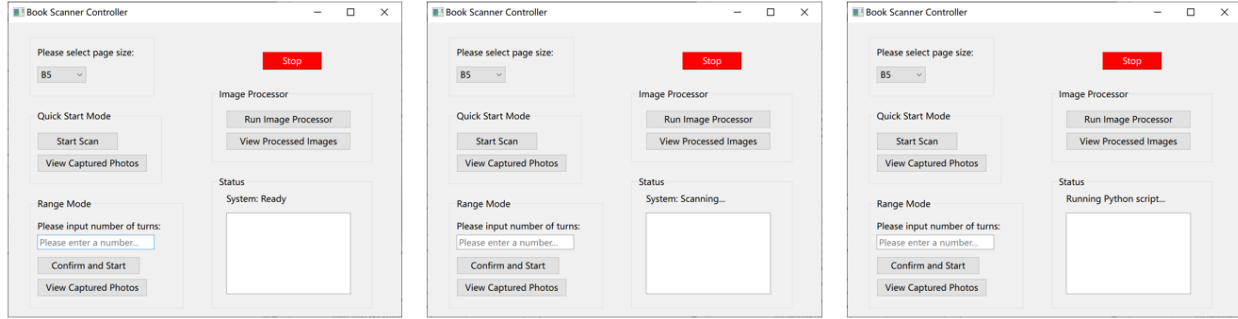


Figure 11: User Interface of Three Different States

These results confirm that the user interface successfully provides feedback to the user and allows effective control of the system, fulfilling its role as an accessible and functional front end for the image processing workflow.

3.2.2 Image Processor

To verify the processing speed of the image processor, we measured the time required to process 10 pages. The average total processing time was recorded as 27.15 seconds, yielding an average of 2.715 seconds per page, which meets the design requirement of ≤ 3 seconds per page.

To evaluate dewarping accuracy, we used OpenCV's HoughLines to analyze page skew. We tested 10 process images and the average skew is 1.76° , which meets the requirement. The final output was visually inspected, and the text remained clear and easily readable. Therefore, the processed content meets usability standards.

3.2.3 Camera

The camera system was tested by capturing 25 images during a controlled scan. Each captured image was checked for content integrity and resolution using image metadata. All images were verified to be exactly 1920×1080 pixels and displayed the book content after each page turn. This confirms that the camera module consistently meets resolution requirements.

3.3 Control Module

3.3.1 Motor Driver

To verify the correct generation of PWM signals, we used an oscilloscope to measure the PWM signal generated by STM32F407, which was intended to increase the duty cycle from 40% to 100%. The results showed a linear correlation between input percentage and output duty cycle, varying from 40.8% to 99.6%, closely matching the expected 40 – 100% range. Representative waveform snapshots are shown in Figure 12. The signal frequency remained stable at 2 kHz, with negligible jitter.

To assess GPIO response time, we connected direction control pins on the L298N driver to the STM32F407 GPIO output pins. The motor controlled by the L298N driver runs in a specific direction as expected. Table 4 shows the relationship between the input signal and motor direction.

Measurements indicate that the motor driver responded approximately 4.5 ms after a GPIO edge trigger, meeting the system's real-time requirement of 5 ms.

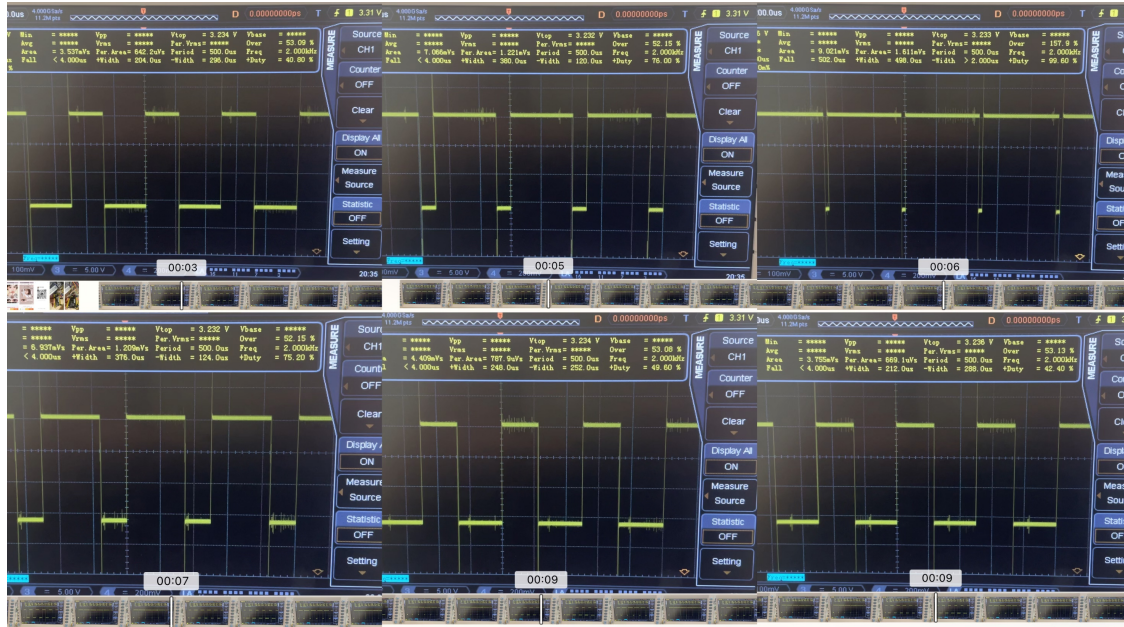


Figure 12: PWM Signal Output on Oscilloscope with Time Label

Table 4: Motor Direction Controlled by Motor driver L298N

| ENA | ENB | IN1 | IN2 | IN3 | IN4 | Motor Performance |
|------------|------------|------|------|------|------|----------------------------|
| 5 V or PWM | X | HIGH | LOW | X | X | Motor A: clockwise |
| 5 V or PWM | X | LOW | HIGH | X | X | Motor A: counter-clockwise |
| X | 5 V or PWM | X | X | HIGH | LOW | Motor B: clockwise |
| X | 5 V or PWM | X | X | LOW | HIGH | Motor B: counter-clockwise |

3.3.2 UART Transmission

To verify the accuracy of UART-based data transmission via CH340, we measured the total transmission time for message sending and receiving by recording a video when

running the Python test script as shown in Figure 13. At a baud rate of 115200 bps, an 80-char message was transmitted in 0.04 seconds. When we tested the UART sending function, from the terminal window, we observed no mismatches between the message sent by STM32F407 and the message received by PC. When we tested the UART receiving function, from the terminal window, we observed no mismatches between the message sent by PC and the message reflected from STM32F407. This indicates reliable transmission with no loss or corruption of byte.

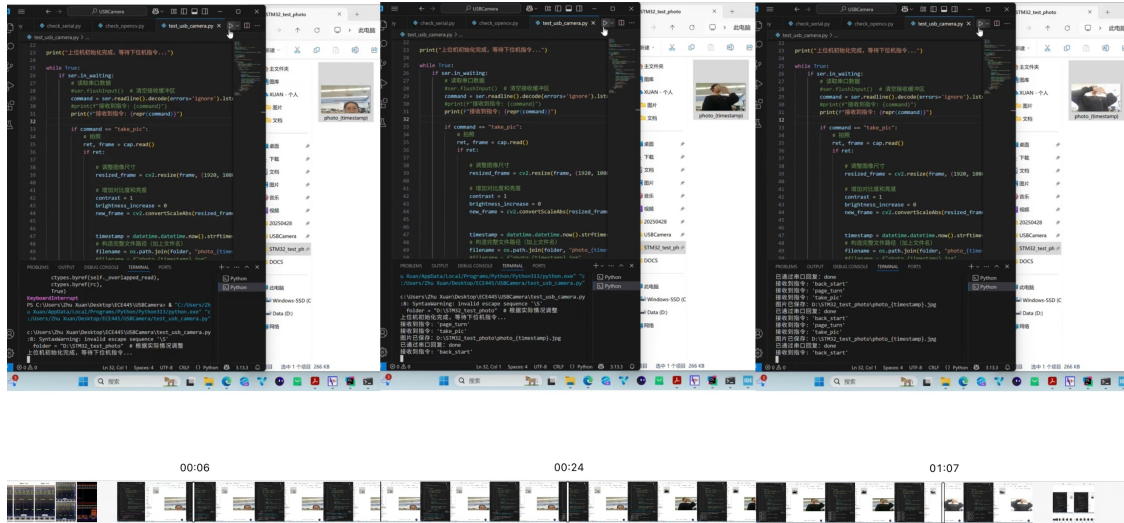
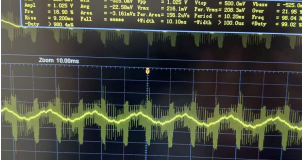




Figure 13: Terminal Window of UART Test with Time Label

3.3.3 Photoelectric Sensor

We conducted a series of experiments and recorded whether a stable zero-voltage phase appeared on the oscilloscope, while also verifying whether the system successfully received and utilized the sensor signal through code execution. The logic of the test program was as follows: during each page-turning process, when the book page blocked the propagation path of the infrared beam and the voltage transitioned from a fluctuating state to a stable zero, the motor controlling the roller would immediately stop rotating. A total of 20 page-turning experiments were carried out. In all 20 trials, a stable zero-voltage phase was observed on the oscilloscope, and the roller motor stopped functioning each time following the voltage drop to zero. In each trial, the period of stable zero-voltage phase is about 30 ms which is shown in Table 5.

Table 5: Page Sensor Test Result

| | |
|---|--|
|  | <p>When the infrared signal emitted by the sensor successfully reaches the receiver, the oscilloscope shows that the voltage is fluctuating.</p> |
|  | <p>When the turning of a book page obstructs the transmission of the infrared beam, the receiver fails to detect the signal, and the oscilloscope registers zero voltage across the sensor.</p> |
|  | <p>During the process of a page being turned, the oscilloscope displays a fluctuating voltage signal, with a short interval of stable zero voltage, indicating that the infrared beam was momentarily obstructed as the page passed through its path. The subsequent resumption of voltage fluctuations signifies that the page has completed its turn and no longer blocks the infrared transmission.</p> |

3.3.4 Emergency Stop

The emergency stop mechanism can be triggered by receiving a specific "STOP" message configured for EXTI from the host PC by clicking the UI button. We measured the time interval between the UI button press and the execution of the interrupt service routine by recording a video. When the emergency stop button was activated, all active PWM outputs controlling the page-separating and page-turning motors were immediately disabled. The response time was consistently within 8 ms, which is below the 10 ms safety threshold.

Following emergency stop activation, the system entered a locked safety mode. Attempts to resume operation without pressing a manual reset button on the STM32F407 board were intentionally blocked by firmware-level state control.

4 Costs

The labor cost is estimated as ¥ 24/hour and 5 hours per week for 4 persons. The overall working weeks for the final design are considered to be 14 weeks.

$$Cost_{manual} = 4 \times 24 \times 5 \times 14 = ¥6720$$

The cost of all components is listed in Table 6. Through enumeration and calculation of the components one by one, it can be confirmed that the material cost is well controlled within the budget.

Table 6: Components Price List

| Part | Description | Price (¥) | Qty | Total (¥) |
|------------------|---------------|-----------|-----|-----------|
| JGB37-520 motor | 12V | 25.00 | 3 | 75.00 |
| Power supply | 220V to 12V | 37.00 | 1 | 37.00 |
| Hinge | JY263AL-B | 11.50 | 2 | 23.00 |
| Bolt and nut | M5 | 0.27 | 20 | 5.40 |
| Bracket | M5,2020 | 1.30 | 15 | 19.50 |
| Hollow cylinder | ϕ 25, 1m | 10.56 | 0.2 | 2.11 |
| Screw rod | 100mm | 294.00 | 1 | 294.00 |
| Bearing | – | 2.75 | 2 | 5.50 |
| Gear chain | – | 53.00 | 1 | 53.00 |
| Aluminum profile | 2020 | 14.00 | 6 | 84.00 |
| Connector | 3D printing | 0.49 | 7 | 3.43 |
| Wood supporter | laser cutting | 68.00 | 1 | 68.00 |
| Motor driver | L298N | 7.47 | 2 | 14.94 |
| ST-LINK chip | – | 12.69 | 1 | 12.69 |
| STM32 Board | F407ZGT6 | 53.61 | 1 | 53.61 |

The grand total cost for all parts is ¥ 751.45. So for our prototype building, the overall cost is estimated to be ¥ 7471.45. If our design products are put into the market and mass manufactured, the labor cost can be reduced to one percent of the original. Thus, the total cost for one product is ¥ 818.65.

5 Schedule

Table 7 shows each member's weekly schedule.

Table 7: Weekly Work Report of Team Members

| Week | Yingying Gao | Yiying Lyu | Xuan Zhu | Shuchang Dong |
|---------|--|--|---|---|
| 2/24/25 | RFA writing | RFA writing | RFA writing | RFA writing |
| 3/3/25 | Search similar products | Search similar products | PCB design | Learn image processing technology |
| 3/10/25 | Discussion and Project Proposal | Discussion and Project Proposal | Discussion and Project Proposal | Discussion and Project Proposal |
| 3/17/25 | Verify the mechanism feasibility | Verify the mechanism feasibility | Microcontroller research | Image processing experiments |
| 3/24/25 | Purchase materials | 3D printing the component | Firmware flashing | Different filters experiments |
| 3/31/25 | Assemble the base frame | Assemble the camera holder | Control motors | Dewarping experiments |
| 4/7/25 | Design document writing | Design document writing | Design document writing | Design document writing |
| 4/14/25 | Realize the page-turning function | Realize the page-turning function | Firmware flashing | Modify the algorithm |
| 4/24/25 | Improve efficiency of the page-turning mechanism | Modify the CAD model | Design the first version of the PCB | Improve the scanning clarity |
| 4/28/25 | Test the success rate of the page-turning function | Test the success rate of the page-turning function | Fabricate the second version of the PCB | Improve the clarity of image processing |
| 5/5/25 | Integration sub-systems | Integration sub-systems | Integration sub-systems | Integration sub-systems |
| 5/12/25 | Interface module | Interface module | Data transmission protocol | Interface module |
| 5/19/25 | Do final test | Do final test | Do final test | Do final test |

6 Conclusion

6.1 Accomplishments

Currently, the mechanical structure of this automatic page-turning photocopier is capable of achieving a continuous page-turning action cycle. The success rate of single-page turning per single attempt exceeds 75%. Meanwhile, the sensor for detecting the success of page-turning can identify the lifted page with a 99% probability and trigger the subsequent page-turning process. In the photocopying stage of the process, the camera can completely cover the entire spread-out page of the book and take pictures for storage. The stored image data will undergo image processing operations such as segmentation, flattening, and clarification in sequence.

6.2 Uncertainties

Under the existing mechanical conditions, for book pages larger than A4 size in a single sheet, a page-turning failure may occur due to a fold in the paper with a possibility of around 20%. During the page-turning process. Moreover, after turning 10 pages, there's a 30% chance that multiple pages will be driven in a single page-turning operation because the pressure between the book and the rollers is too high, The mechanical structure of the entire instrument needs to be adaptively adjusted according to the size and thickness of different books before starting so that the designated automatic page-turning and photocopying functions for multiple pages can be completed more smoothly.

6.3 Ethical considerations

According to the IEEE Ethics Framework [1], the design needs to have human well-being at its core. Scanners may process sensitive documents, such as personal documents, files, etc. Define the responsibilities of the manufacturer, operator, or maintainer if a device failure results in document damage or data disclosure. Device operation logs are recorded to facilitate fault tracing. The environmental and sustainability aspect is to increase the efficiency ratio of the motor drive system and save energy. Physical safety is limited in the design of mechanical structures to ensure that the operator's body is not harmed. The motor drive parts need to be equipped with protective covers to prevent the user from physical damage.

6.4 Future Work

In the future, the adaptation work for more types of books with different materials and sizes needs to be improved. In terms of control, the page-turning process should be shortened to reduce the time required for a page-turning cycle. In the aspect of image processing, in addition to clarification and saving, a more intelligent text recognition function should be added. Through these improvements, the automatic page-turning photocopier can adapt to more archival work and provide users with better and more user-friendly services.

References

- [1] I. of Electrical and E. Engineers, *Ieee code of ethics*, <https://www.ieee.org/about/corporate/governance/p7-8.html>, Accessed: 2025-4-13, 2020.
- [2] P. P. Authority, *Page-dewarp*, <https://pypi.org/project/page-dewarp/>, Accessed: 2025-4-13, 2025.
- [3] L. M. Meyer, *Document image dewarping library using a cubic sheet model*, <https://github.com/lmmx/page-dewarp>, Accessed: 2025-4-13, 2023.
- [4] Mikumiku339, *Python image processing: Document photo scanning (manually building a scanner)*, <https://blog.csdn.net/Mikumiku339/article/details/114766705>, Accessed: 2025-4-13, 2021.
- [5] STMicroelectronics, *Rm0090 reference manual: Stm32f405/415, stm32f407/417, stm32f427/437 and stm32f429/439 advanced arm[®]-based 32-bit mcus*, <https://www.st.com>, Accessed: 2025-4-13, 2021.

Appendix

Table 8: Requirements and Verification of Page-Turning Module

| Requirements | Verifications |
|--|---|
| <ol style="list-style-type: none"> 1. The drum must reliably separate individual pages via friction without adjacent page interference. 2. Achieve $\geq 80\%$ success rate over 10 consecutive cycles (≤ 2 failures). It should have material compatibility, supporting diverse paper types. 3. The time cost should be as short as possible. 4. Correctly identify page-turning events with $\leq 2\%$ false positives (non-page triggers) and $\leq 1\%$ missed detections. 5. Voltage signal transition 10–90% must complete within ≤ 10 ms after page interruption. 6. Telescopic rod must enable vertical (200–800 mm) adjustments with ± 2 mm repeatability. 7. The book platform must support ≤ 2 kg static load without deformation. | <ol style="list-style-type: none"> 1. Conduct 10 tests on more than 2 types of papers and record the success rate. 2. Record full page-turning cycles (separation to completion) which take no more than 20 seconds. Adjust the speed of motors to make an efficient page-turning cycle. 3. Test whether the system can judge page turning from the output signal of the page sensor and conduct 20 times page turns and record detection results system judges. 4. Conduct page turning process multiple times and use an oscilloscope to capture signal rise/fall times during controlled page interruptions. 5. Put books with diverse sizes on the book platform and adjust the angle of the hinge to prevent page distortion and occlusion. Conduct vertical adjustments to make sure that the full range of books could be captured. 6. Put books with diverse weights (0.1-0.6 kg) on the book platform for 2 hours. Measure the deformation of the component that supports the book platform via the vernier caliper. |

Table 9: Requirements and Verification of Image Processing Module

| Requirements | Verifications |
|--|---|
| <ol style="list-style-type: none"> 1. Image processor must process each page in ≤ 3 seconds at 300 DPI. 2. Image processor must dewarp pages to a flat plane with $\leq 2^\circ$ skew. 3. The camera must capture one image with a resolution of 1920×1080 pixels each time the book is turned. 4. The user interface must allow users to initiate a scan using the "Start Scan" button and to stop the scan using the "Stop" button. 5. The user interface must trigger the image processor via the "Run Image Processor" button. 6. In range mode, the system accurately turns the exact number of pages specified by the user via the user interface. 7. The user interface must display real-time system status updates. | <ol style="list-style-type: none"> 1. Record the processing time for 10 pages and check the processing time. 2. Verify the average skew of 10 processed images via software (e.g., OpenCV's HoughLines). 3. Verify that the saved images match the book pages and their resolution is 1920×1080. 4. Press "Start Scan" and verify all activity begins within 1 second. Then press "Stop" and verify all activity halts within 1 second. 5. Click "Run Image Processor" and verify that processed images are generated and stored in the appropriate folder. 6. Input 10 distinct numbers and verify through observation that the system performs the corresponding number of page turns accurately. 7. Trigger system state changes (e.g., scan start, image processing) and verify that the status display updates within 500 ms of event initiation. |

Table 10: Requirements and Verification of Control Module

| Requirements | Verifications |
|--|--|
| <ol style="list-style-type: none"> 1. Motors must operate directionally with adjustable speed between 0–100% duty cycle. 2. Motors must support both forward and reverse rotation with direction switching within 5 ms. 3. Data must be transferred over UART to a host PC at 115200 bps without frame corruption. 4. The system shall detect a low GPIO signal from the photoelectric sensor once an item passes through the beam path. 5. Emergency stop must trigger an interrupt, and the system must remain halted until a manual reset or power cycle is performed. | <ol style="list-style-type: none"> 1. Measure PWM duty cycle output and confirm it can be varied by the user via an oscilloscope. 2. Observe motor behavior and confirm that direction switching is responsive within 5 ms of GPIO signal change. 3. Measure UART transmission time and confirm correct data reception via checksum validation on the host PC. 4. Verify via oscilloscope that a stable low GPIO signal occurs during each page turn. 5. Simulate emergency stops during operation and verify that the system halts immediately and consistently. |

Figure 14: Schematic of Microcontroller

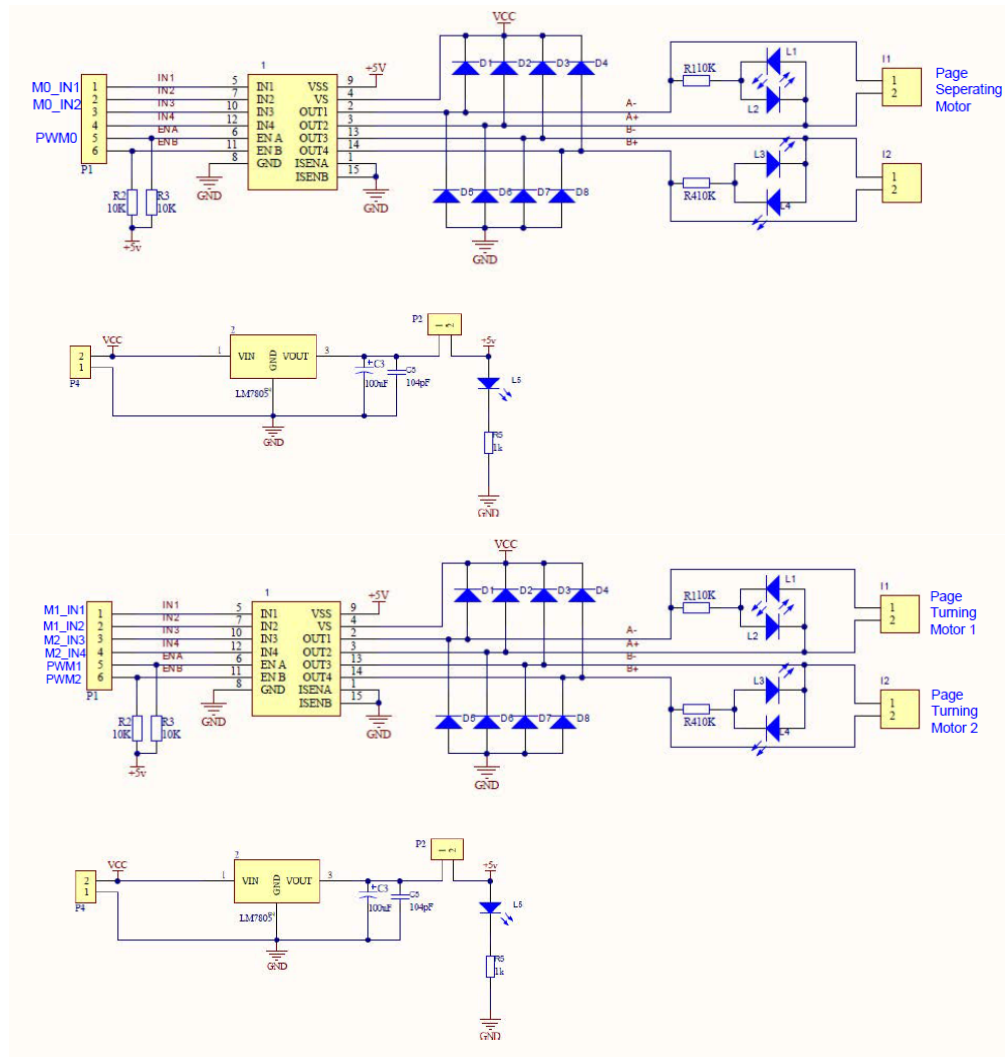


Figure 15: Schematic of Motor Driver

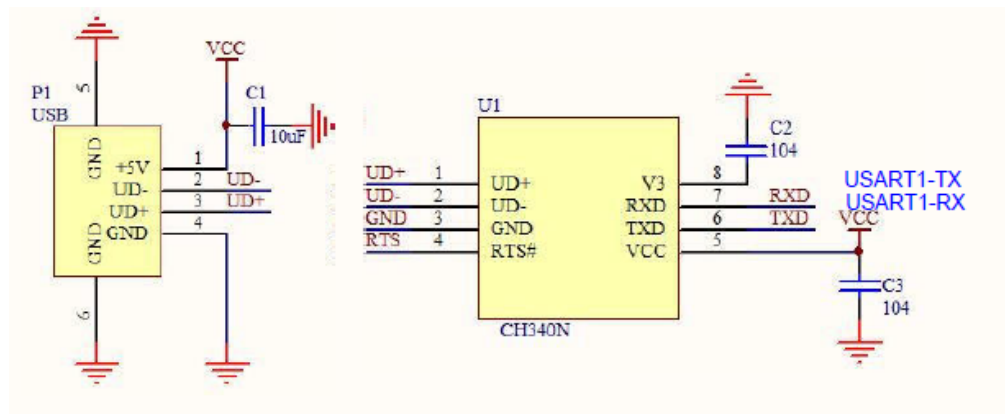


Figure 16: Schematic of USART

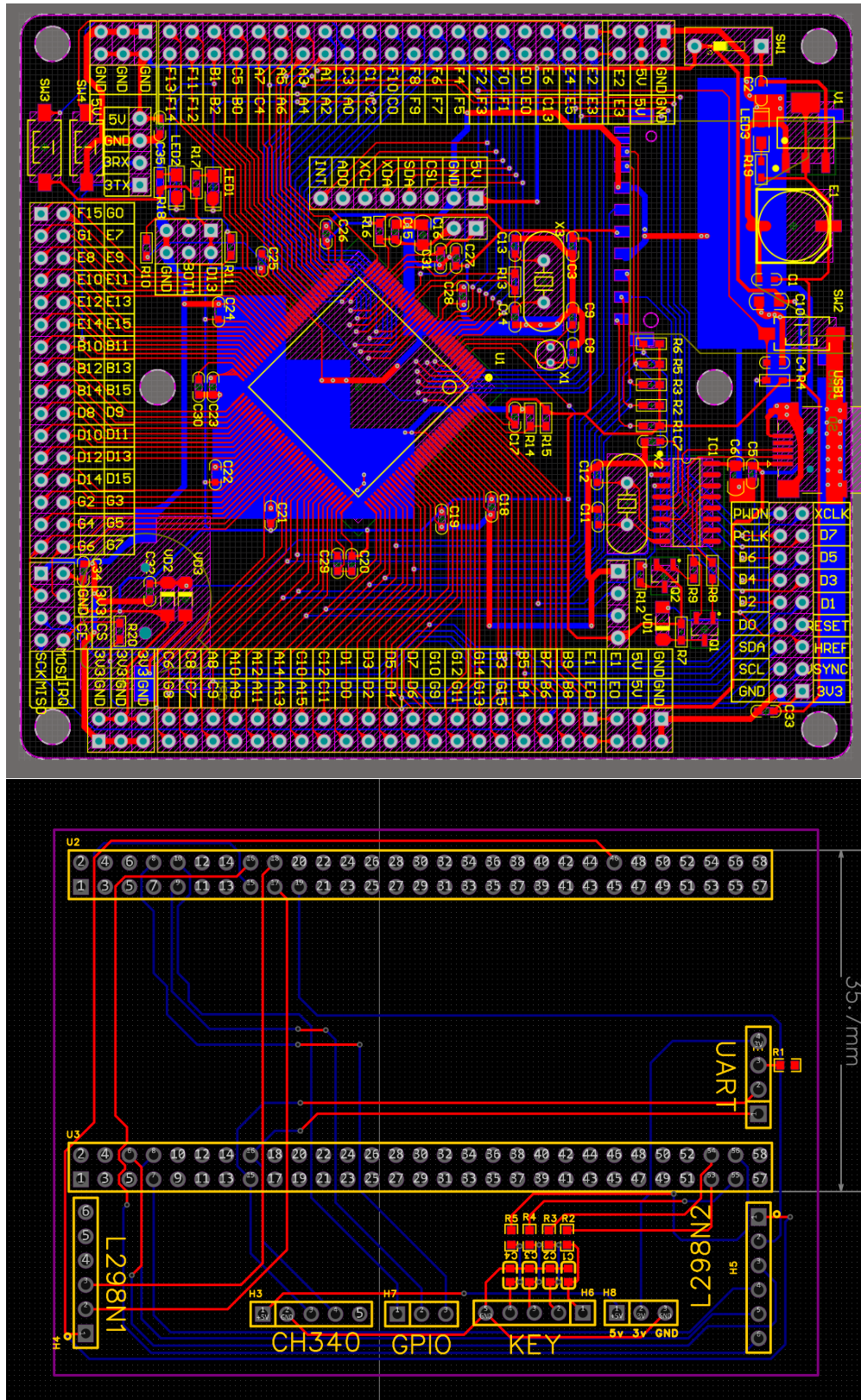


Figure 17: PCB Layout